

## Effect of powder processing conditions on the electromechanical properties of lithium doped potassium sodium niobate



Ebru Mensur-Alkoy<sup>a,\*</sup>, Ayse Berksoy-Yavuz<sup>b</sup>

<sup>a</sup> Faculty of Engineering and Natural Sciences, Maltepe University, Istanbul 34857, Turkey

<sup>b</sup> Department of Materials Science and Engineering, Gebze Technical University, 41400, Turkey

### ARTICLE INFO

#### Article history:

Received 28 January 2016

Accepted 22 April 2016

Available online 11 May 2016

#### Keywords:

Potassium sodium niobate

Piezoelectrics

Strain

Lead-free

### ABSTRACT

Lithium doped potassium sodium niobate ceramics with  $(K_{0.50-x/2}Na_{0.50-x/2}Li_x)NbO_3$  composition where  $x=0.04$  and  $0.07$  were fabricated by solid state calcination and pressureless sintering methods. However, two different powder processing and calcination routes were used in this study and their effect on the structural and electrical properties were investigated and discussed. The routes were namely loose calcination and compact calcination. A general trend of decreasing grain size was observed in the sintered ceramics prepared from these powders. The most drastic effect was observed on the electromechanical properties of the samples, where the maximum strain of 7% lithium modified sample under an  $E$ -field of  $50\text{ kV/cm}$  was increased from 0.09% to 0.12% by changing processing route. Furthermore, hysteretic behavior of the strain was found to decrease. This tendency was also valid for ferroelectric hysteresis property, with remnant polarization ( $2P_r$ ) increasing from  $23\text{ }\mu\text{C/cm}^2$  to  $46\text{ }\mu\text{C/cm}^2$ . The improvements observed in the electrical properties were discussed on the basis of chemical homogeneity and uniform ionic distribution.

© 2016 SECV. Published by Elsevier España, S.L.U. This is an open access article under the CC BY-NC-ND license (<http://creativecommons.org/licenses/by-nc-nd/4.0/>).

## Efecto de las condiciones de procesamiento de polvo en las propiedades electromecánicas del niobato de sodio y potasio dopado con litio

### RESUMEN

#### Palabras clave:

Niobato de sodio y potasio

Piezoelectrónico

Tensión

Sin plomo

Cerámicas de niobato de sodio y potasio dopado con litio con la composición  $(K_{0.50-x/2}Na_{0.50-x/2}Li_x)NbO_3$ , donde  $x=0.04$  y  $0.07$ , se fabricaron por calcinación de estado sólido y métodos de sinterización sin presión. Sin embargo, en este estudio se utilizaron 2 vías diferentes de procesamiento de polvo y calcinación, y se investigó y discutió su efecto sobre las propiedades estructurales y eléctricas. Las vías concretamente fueron calcinación suelta y calcinación compacta. Se observó una tendencia general de disminución de tamaño del grano en la cerámica sinterizada, preparada a partir de estos polvos. El efecto más drástico se observó en las propiedades electromecánicas de las muestras, donde la tensión máxima del 7% de la muestra de litio modificado bajo un campo eléctrico de  $50\text{ kV/cm}$  se incrementó del 0,09 al 0,12% al cambiar la vía de procesamiento. Además, se observó que disminuía

\* Corresponding author.

E-mail addresses: [ebrualkoy@maltepe.edu.tr](mailto:ebrualkoy@maltepe.edu.tr), [ebrualkoy@gmail.com](mailto:ebrualkoy@gmail.com) (E. Mensur-Alkoy).

<http://dx.doi.org/10.1016/j.bsecv.2016.04.005>

0366-3175/© 2016 SECV. Published by Elsevier España, S.L.U. This is an open access article under the CC BY-NC-ND license (<http://creativecommons.org/licenses/by-nc-nd/4.0/>).

el comportamiento histerético de la tensión. Esta tendencia también fue válida para la propiedad de histéresis ferroeléctrica, con polarización remanente ( $2P_r$ ), que aumentó de 23 a  $46 \mu\text{C}/\text{cm}^2$ . Las mejoras observadas en las propiedades eléctricas se discutieron sobre la base de la homogeneidad química y la distribución iónica uniforme.

© 2016 SECV. Publicado por Elsevier España, S.L.U. Este es un artículo Open Access bajo la licencia CC BY-NC-ND (<http://creativecommons.org/licenses/by-nc-nd/4.0/>).

## Introduction

There has been a big drive in last fifteen years to develop lead-free materials with properties that are comparable to the lead-based ones for commercial piezoelectric applications [1]. Among the lead-free candidates, the potassium sodium niobate –  $(\text{K}_{0.50}\text{Na}_{0.50})\text{NbO}_3$  (KNN) is considered to be promising due to its high Curie temperature and piezoelectric properties [1–6]. However, it is well known that KNN produced by conventional sintering methods has complex densification problems which, in turn, affect the electrical properties. This can be improved by various sintering aids, or non-conventional sintering methods, such as hot pressing or spark plasma sintering [2–7].

There have also been some studies to find new systems based on KNN that can be sintered by conventional pressureless method [3–9]. In the current study, lithium (Li) substitution is the main approach where the composition is  $(\text{K}_{0.50-x/2}\text{Na}_{0.50-x/2}\text{Li}_x)\text{NbO}_3$ . Lithium ratio was chosen as  $x=0.0, 0.04$  and  $0.07$  [1,3,6,9]. The KNN has  $\text{ABO}_3$  perovskite structure and  $\text{Li}^+$  assumes the A-site position as an isovalent substitution.  $\text{Li}^+$  has a small ionic radius compared to  $\text{Na}^+$  and  $\text{K}^+$ , thus the Li doping will affect the unit cell of the KNN, as well as the polarizability of the structure. Additionally, lithium niobate ( $\text{LiNbO}_3$ ) is a typical ferroelectric material with trigonal structure and a high Curie temperature ( $1142^\circ\text{C}$ ). Thus, it was reported that phase transition temperatures shifted with Li doping [3,6,10,11]. This high Curie temperature is advantageous for practical applications. The temperature of the transition between two ferroelectric phases (orthorhombic-tetragonal) can also be adjusted through the amount of Li doping. This in turn improves the room temperature piezoelectric properties [1,12].

One of the main applications of lead-free piezoelectrics would be the actuators. Actuators are described as transducers capable of transforming input electrical energy into a mechanical energy. Actuators and high precision positioning systems require high strain levels with high force. They are mainly designed for maximum strain at minimum coercive electric field ( $E_c$ ). Electric field induced strain ( $S_{ij}$ ) can be described with the following equation:

$$S_{ij} = d_{kij}E_k + M_{ijkl}E_kE_l + \dots \quad (i, j, k) = 1, 2, 3 \quad (1)$$

where the first term in this equation represents the contribution of the converse piezoelectric effect, and the second term contains the electrostrictive contribution. The linearity of strain with respect to the applied electric field is valid only for low levels of electric field, and thus, it is called as the small-signal property. The piezoelectric charge coefficient ( $d_{ij}$ ) (or

specifically  $d_{33}$ ) is normally measured or calculated for this region [13]. The high-field converse piezoelectric charge coefficient  $d_{33}^*$  on the other hand is called the large-signal quantity and hence in ferroelectrics includes strain contributions by domain switching. The high-field converse piezoelectric coefficient can be calculated from the maximum value of strain and electric field as  $d_{33}^* = S_3/E_3$  for applications. In fact,  $d_{33}^*$  is an important figure of merit which is similar to the direct piezoelectric charge coefficient  $d_{33}$ .

The aforementioned reasons to incorporate  $\text{Li}^+$  into the perovskite KNN structure are well established and have been discussed and investigated in the literature [1–12]. The original contribution of this paper to the literature and the main difference from our previous published work is the observation of a drastic effect of the powder processing method, which we have used in our process, on the electromechanical properties of the ceramics [3,6,12].

## Experimental

All the ceramic samples were prepared using conventional solid state calcination method. Potassium carbonate ( $\text{K}_2\text{CO}_3$ ), sodium carbonate ( $\text{Na}_2\text{CO}_3$ ), niobium oxide ( $\text{Nb}_2\text{O}_5$ ) and lithium oxide ( $\text{Li}_2\text{O}$ ) (Aldrich, USA) were used as starting powder materials. The main composition was chosen as  $(\text{K}_{0.50-x/2}\text{Na}_{0.50-x/2}\text{Li}_x)\text{NbO}_3$ . The green powders in  $(\text{K}_{0.50-x/2}\text{Na}_{0.50-x/2}\text{Li}_x)\text{NbO}_3$  composition were mixed by ball-milling with aid of  $\text{ZrO}_2$  balls in ethanol for 24 h with K:Na ratio of 1:1.

Two different calcination routes were used to prepare the ceramic powders. In the first calcination method that is named as the ‘loose-calcination’ and referred to in the text as R1, the mixing step by ball-milling was followed by drying the green powder mixture on a hot plate while continuously stirring using a magnetic stirrer. Then the dried green powders were put into an alumina crucible as a loose powder and calcined. This was the procedure that we have followed in our previous studies on KNN [7,9–11]. Calcined powders were again ball-milled for 24 h. The Li content was  $x=0.04$  and  $0.07$  with the samples produced with R1 and they were named as KL4 and KL7, respectively. This naming convention is the same with our previous studies [9,11].

On the other hand, in the new calcination method that is named as the ‘compact-calcination’ and referred to in the text as R2, disc-shaped samples were prepared from the dried powder mixture by dry pressing under a uniaxial pressure of 55 MPa. These disc samples were then calcined instead of calcining loose powders. After calcination, samples were crashed using mortar and pestle. The crashed powders were again ball-milled for 24 h. The Li content was  $x=0.04$  and  $0.07$  with

the samples produced by R2 and named as L4 and L7, respectively.

Calcination of all the samples in both of the calcination routes was done at 900 °C for 1 h. After the calcination process, disc-shaped samples with ~10.5 mm diameter and ~1 mm thickness were prepared by pressing under a uniaxial pressure of 100 MPa and then sintered at 1090 °C for 1 h. Finally, silver-palladium electrode was applied to the parallel surfaces of the discs for electrical measurements, and annealed at 850 °C for 30 min.

Structural analysis of the powders and sintered samples was done by X-ray diffraction (XRD) method (Bruker D8 Advanced, Bruker AXS GmbH, Germany 2200) using Cu K $\alpha$  radiation. Scanning electron microscope – SEM (XL30, FEI, USA) was used to examine the microstructural features of the samples. Polarization vs. electric field hysteresis loops and electric field induced strain behavior of the samples were measured using a ferroelectric tester (Precision LC Ferroelectric Tester, Radiant Technologies, USA) and a photonic sensor (MTI 2000, MTI Instruments Inc., USA).

## Results and discussion

In our previous studies [9–11], structural features of lithium modified ( $(K_{0.50-x/2}Na_{0.50-x/2}Li_x)NbO_3$ ) samples were reported in detail. However, these results have not been used in this study and all Li modified samples were prepared again for this study by R1 and R2 methods. It was seen from XRD patterns taken at room temperature (Fig. 1) that peak intensity of 4% Li modified sample prepared by R2 method (L4) is higher than that of KL4 sample (prepared by R1) (Fig. 1(a) and (b)). This indicates that L4 sample has higher crystallinity compared to KL4. There was no additional difference between KL4 and L4. A similar result was also observed from XRD analysis of KL7 and L7 samples. The additional small intensity peaks that were observed at  $2\theta$  from 25° to 30° belong to a secondary  $K_6Li_4Nb_{10}O_{30}$  phase (JCPDS card No. 48-0997), that was reported [14] to be observed due to volatilization of Na at temperatures above 1100 °C.

The XRD peaks around 45–46° were investigated in detail and presented in Fig. 1(b). From this figure, it was concluded that while L4 sample ( $x=0.04$ ) exhibits a (202)/(020) peak splitting which belongs to the orthorhombic symmetry, L7 ( $x=0.07$ ) exhibits (002)/(200) peak splitting which confirms the tetragonal structure. One striking results in this comparison is the increasing peak splitting in the (002)/(200) peaks of the L7 sample compared to the KL7 sample. This increasing splitting indicates an increasing tetragonality of the structure with the R2 compact-calcination method. The observance of XRD peaks belonging to the tetragonal symmetry in the case of 7 mol% Li addition and that of orthorhombic symmetry in the case of 4 mol% Li addition are compatible with our previous report [10] and some other reports in the literature [2,6]. Thus, changing the calcination method does not lead to a change in the crystal symmetry of the samples, as expected. These results were also confirmed by temperature dependent dielectric constant ( $K$  vs.  $T$ ) measurements shown in Fig. 3(d) and they are also consistent with the literature [9–11,15]. Orthorhombic to tetragonal phase transition ( $T_o$ ) temperature was around 140 °C for L4

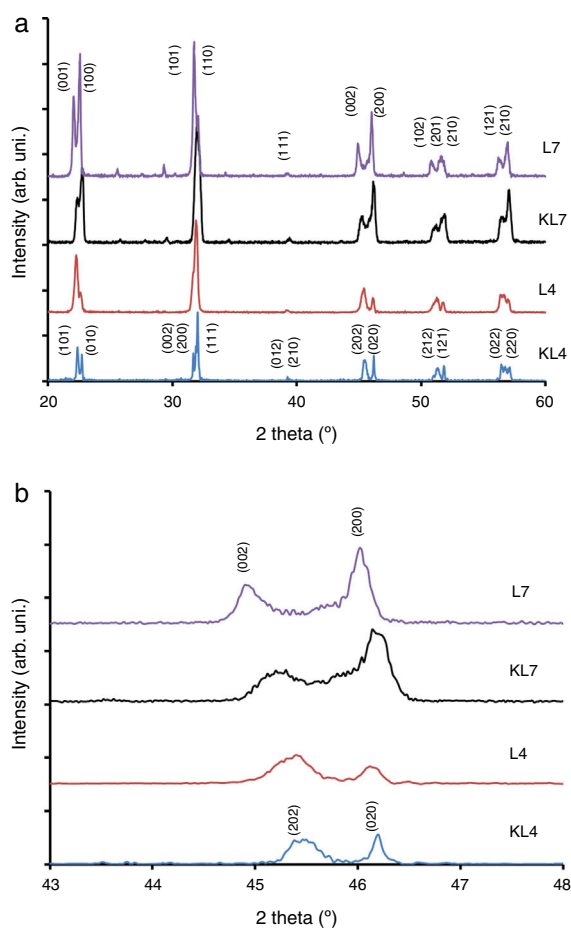


**Fig. 1 – XRD patterns of (a) KL4, L4, KL7 and L7 samples, and (b) XRD patterns of selected region of the same samples. The peaks of KL4 and L4 were indexed based on the perovskite structure with orthorhombic symmetry and the peaks of KL7 and L7 were indexed based on the tetragonal symmetry.**

sample, which indicates orthorhombic phase at room temperature [9,15]. This transition peak was not observed for L7 sample down to room temperature, as shown in Fig. 3(d). This also indicates that L7 composition has tetragonal symmetry at room temperature.

From the XRD investigations, it is safe to conclude that R2 compact-calcination is a preferable method for better crystallinity. Increasing crystallinity in the case of 4 mol% Li and increasing tetragonality in the case of 7 mol% Li addition indicate that the calcination method has a positive effect on the structural properties of the powders and on the resultant sintered ceramics in return.

The microstructures of the sintered samples were also investigated by scanning electron microscope (SEM) and a clear and drastic difference was observed between the grain sizes and morphology of the samples produced by modified fabrication method R2 and conventional method R1 (Fig. 2). All ceramics have dense microstructures with bimodal grain size distribution regardless of the calcination method. The microstructures of the samples produced by R1 have also been discussed in our papers [9–11]. It is known that increasing

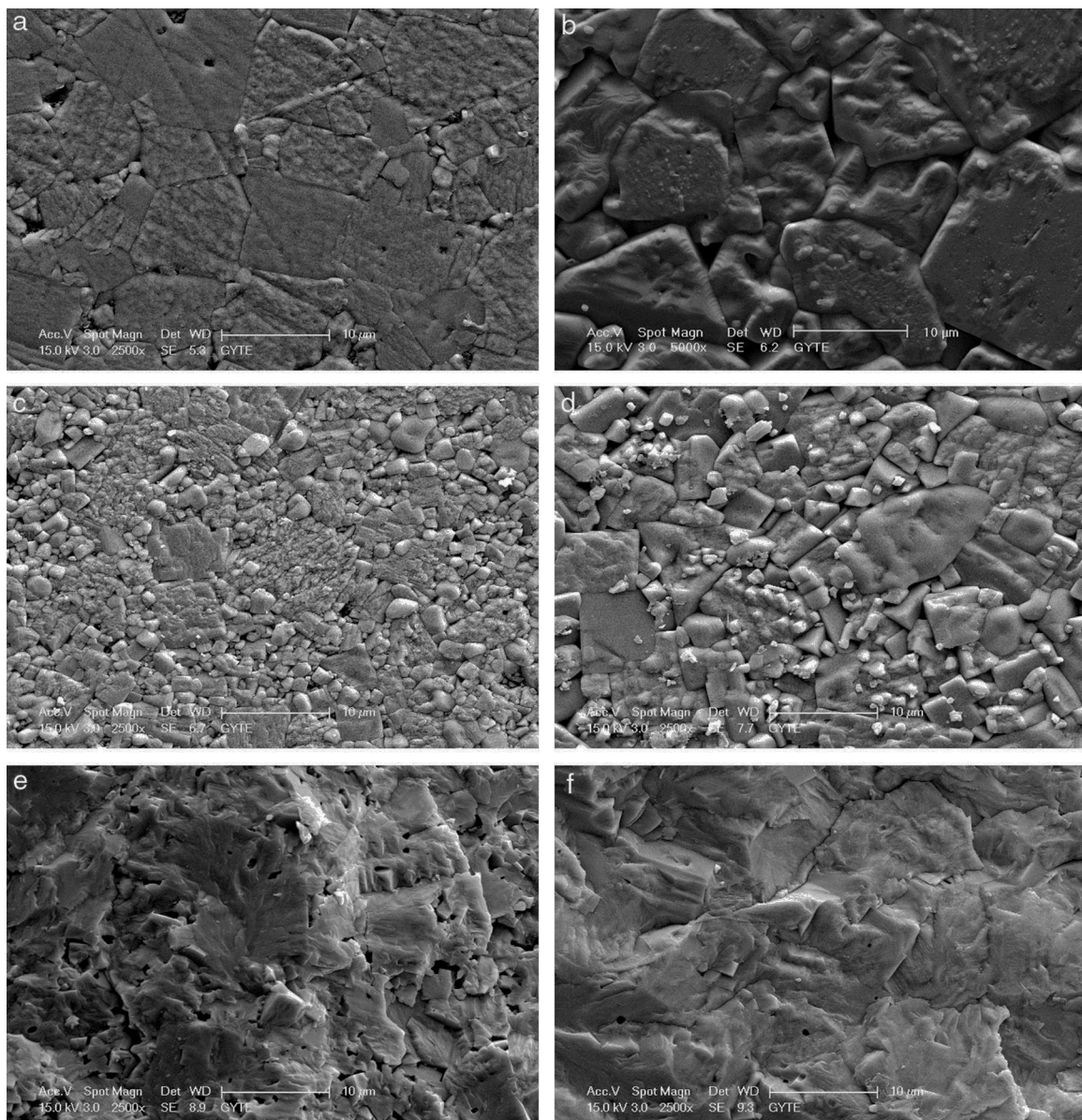


**Fig. 2 – The SEM micrographs of (a) KL4, (b) KL7, (c) L4 and (d) L7 samples. Fracture surface micrographs of (e) L4 and (f) L7 sample.**

lithium ratio in the structure promotes grain growth [6,16] and this has also been observed and reported by our group [10]. In the current case, it is clearly seen that increasing the Li content from 4 mol% to 7 mol% again promotes grain growth, as shown in Fig. 2(a) and (b) for R1 method and in Fig. 2(c) and (d) for R2 method. Grain size of KL4 and KL7 samples were calculated from SEM micrographs using line intercept method as  $\sim 7.3 \mu\text{m}$  and  $\sim 9.4 \mu\text{m}$ , respectively. But the more dramatic result is that the grain sizes of the both 4% and 7% Li modified samples prepared through the R2 method (Fig. 2(c) and (d)) are drastically smaller than the ones prepared through the R1 method (Fig. 2(a) and (b)). Grain size of L4 and L7 samples was calculated as  $\sim 3.3 \mu\text{m}$  and  $\sim 5.7 \mu\text{m}$ , respectively. It may be possible to explain these smaller grain sizes in the R2 method based on the absence of liquid phases. The loose-calcination

(R1) method causes incomplete mixing of the constituents and incomplete reactions which may lead to formation of liquid phases at the sintering temperatures. This may in turn lead to abnormal grain growth due to easier diffusion and grain growth in the presence of a liquid phase. Whereas, the compact-calcination (R2) method is expected to yield a more homogeneous and uniform mixture of the constituents, and thus, liquid phases may not appear. This will result in a sintered microstructure with regular grains.

The fracture surfaces of the samples prepared by R2 method are also given in Fig. 2(e) and (f) and they confirm the dense microstructure of the samples. As an overall conclusion of structural part of this study, increasing crystallinity and decreasing grain size were the two most important results obtained as a result of R2 calcination route. Structure–property

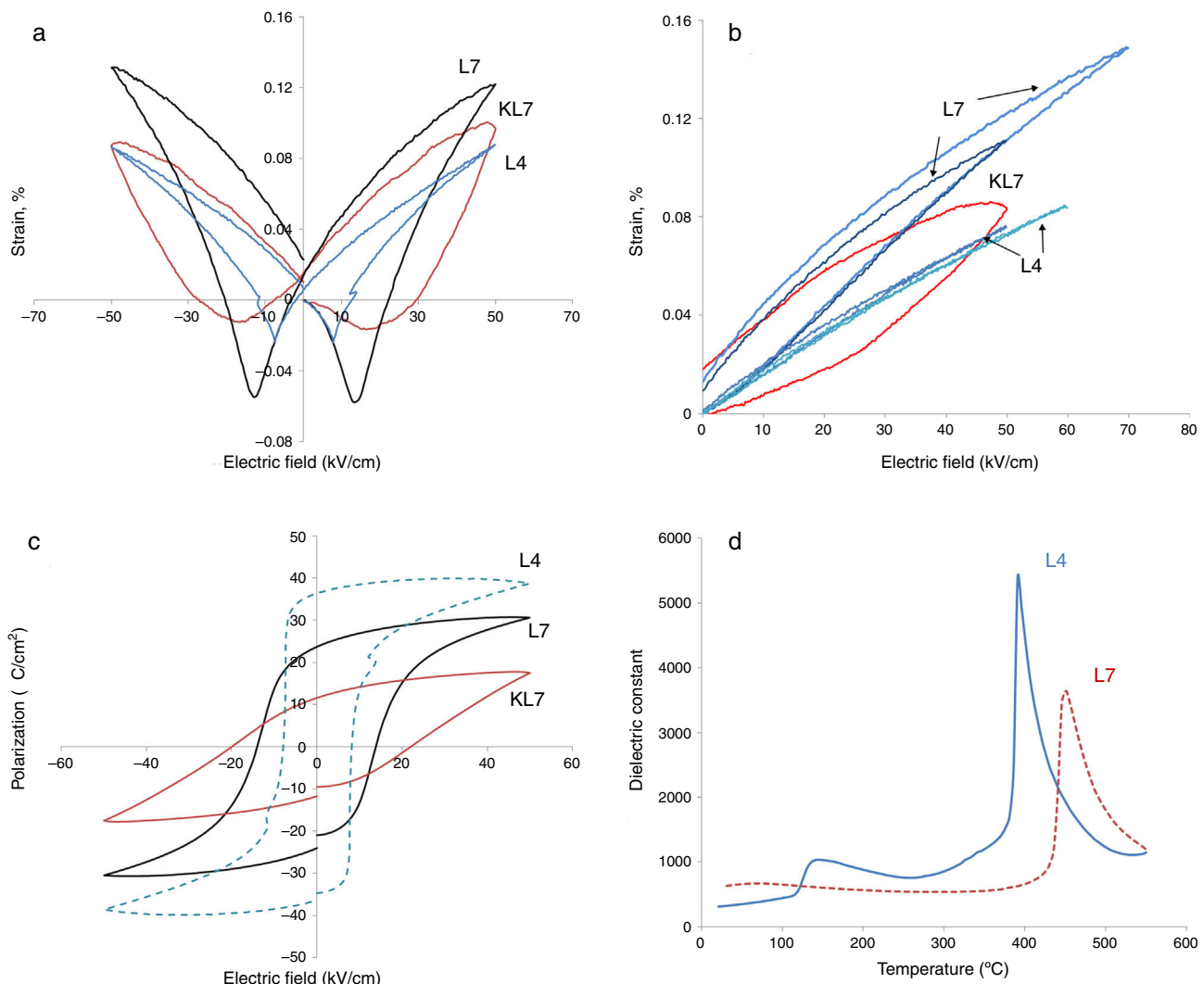


**Fig. 3 – Comparison of (a) bipolar strain, (b) monopolar strain and (c) polarization vs. hysteresis of 4 and 7 mol% Li modified L4, KL7 and L7 samples. (d) Comparison of the temperature dependent dielectric constant of L7 and L4 samples.**

relationships were investigated and discussed in the light of these results.

Electrical measurements were made on ceramics with densities that were >96% of the theoretical value. Electromechanical and ferroelectric properties were investigated to establish a processing–structure–property relationship in Li-doped KNN ceramics. The bipolar and unipolar field induced strain and polarization were measured at room temperature under a triangular waveform with 100 Hz frequency. The results are presented in Fig. 3.

In our previous studies, strain levels of 7 mol% Li modified KNN prepared by the conventional pressureless method (R1), i.e. KL7 in this study as was mentioned before, was reported as 0.1% with hysteretic behavior and this level was comparable to the literature [9]. Coercive field was around 20 kV/cm. The calculated value of  $d_{33}^*$  for that sample was reported as 165 pm/V (picometers/Volt) [9]. In the current study, big differences on the electrical properties, especially on the electromechanical properties, were obtained after the processing method of samples was changed to R2, as seen in Fig. 3. In Fig. 3(a), the

comparison of electric field induced bipolar strain properties of 7 mol% Li modified KNN samples taken at 50 kV/cm (KL7 and L7) are given. The data taken from L4 sample produced through the R2 method has also been included in this figure. All three of the samples display butterfly strain curves with a negative strain region. Increasing Li content from 4 mol% to 7 mol% was definitely effective on the electromechanical properties, which is rather expected. However, it is also clear that processing method was effective on the electromechanical properties. L7 sample has a less hysteretic behavior and higher strain levels when compared to that of KL7 sample. This is believed to be due to the more homogeneous distribution of K<sup>+</sup>, Na<sup>+</sup> and Li<sup>+</sup> ions and obtaining a better stoichiometry through the R2 calcination method. In the literature, distribution of Zr<sup>4+</sup>, Ti<sup>4+</sup> and La<sup>3+</sup> ions during the processing of lead zirconate titanate ceramics was investigated and three types of inhomogeneities was detected in conventionally prepared PZT ceramics; namely Ti and La enriched regions in the core of PZT grains, PbO-rich secondary phases in triple junctions and grain boundary films [17]. These inhomogeneities were

reported to affect the sintering behavior of the PZT ceramics, however, their effect on the electrical properties have not been reported. In another study in the literature, distribution of  $\text{Ca}^{2+}$  ions in the  $\text{Ba}_{0.9}\text{Ca}_{0.1}\text{TiO}_3$  structure was studied using two different powder synthesis routes and the effect of uniform distribution and chemical homogeneity on the dielectric properties have been discussed [18]. Better chemical homogeneity in terms of  $\text{Ca}^{2+}$  ion distribution was found to lead to a more pronounced diffuse phase transition in the  $\text{Ba}_{0.9}\text{Ca}_{0.1}\text{TiO}_3$ .

In our case, the KNN powders were prepared from potassium carbonate ( $\text{K}_2\text{CO}_3$ ), sodium carbonate ( $\text{Na}_2\text{CO}_3$ ), niobium oxide ( $\text{Nb}_2\text{O}_5$ ) and lithium oxide ( $\text{Li}_2\text{O}$ ). A homogeneous and intimate mixture of these powders has utmost importance in the uniform distribution of  $\text{K}^+$ ,  $\text{Na}^+$  and  $\text{Li}^+$  ions and in obtaining the relevant phases in the desired stoichiometry. Normally, hysteresis may arise due to point defects and space charges related to oxygen vacancies. In the case of Li-doped KNN, replacing  $\text{K}^+$  or  $\text{Na}^+$  with  $\text{Li}^+$  would be an isovalent substitution and is not expected to create an additional point defect, or is not expected to cause additional space charges. However, the R1 method is expected to lead to an insufficient mixture of the constituents, and thus, may result in formation of compositional gradients due to different volatility of these constituent phases. Deviations from the stoichiometry are known to cause point defects in the perovskite structure and affect the electrical properties. Thus, it is our initial conclusion that chemical homogeneity and uniform distribution of ions in the structure is the key point in the observed improvements.

When unipolar strain properties of the samples were compared (Fig. 3(b)), similar results were observed. From Fig. 3(b), an additional effect that was observed of the R2 method is that the L7 sample can handle higher electric fields without breakdown compared to KL7. The  $d_{33}^*$  values were calculated as 220, 162 and 152 pm/V under 50 kV/cm electric field for L7, KL7 and L4 samples, respectively. This value was calculated as 120 pm/V for KL4. Additionally, when the unipolar strain behavior of L4 and L7 are compared (see Fig. 3(b)), it was found that the strain level of L7 is much higher compared to L4. Strain level is associated with piezoelectric constants and this in return is related to two sources in the case of Li-doped KNN. The first contribution is from the fact that the orthorhombic to tetragonal transition is lowered to around room temperature. As a result of this phase transition, the piezoelectric activity is increased. Additional source is from the intrinsic contribution to the piezoelectric activity.  $\text{Li}^+$  is a smaller ion compared to  $\text{Na}^+$  and  $\text{K}^+$  [20], thus, a higher polarizability is expected due to the easier mobility of ion in the crystal structure. Another interesting observation in the comparison of the unipolar strain of L4 and L7 is the almost non-existing hysteresis in the L4 sample. This would have its advantages in certain high power applications due to lower losses [21].

Hysteresis vs. electric field behaviors of the 4 and 7 mol% Li modified samples was also measured and the results are given in Fig. 3(c). These measurements were taken simultaneously with the strain measurements. The effect of processing method is more drastic on the P-E behavior. The remnant polarization of L7 is twice that of KL7. The coercive field is also lower with the R2 processing route and it is 13 kV/cm for L7 sample (Fig. 3(c)). Additionally, the P-E hysteresis curve of

KL7 is more slanted, whereas the hysteresis curve of L7 is more square-like. The remnant polarization ( $P_r$ ) is reported to reflect the degree of lattice distortion, and thus it can be considered as a direct indicator for the intrinsic contributions [19]. The level of  $P_r$  obtained in the KL7 is lower than its counterparts in the literature [6], but the  $P_r$  of L7 is comparable. This also emphasizes the close correlation between the processing and the properties. The square-like hysteresis behavior and lower coercive field values in the L7 compared to KL7 is believed to be an indication of a dominant 180° domain switching and it is related to the tetragonality of the sample. From the XRD data shown in Fig. 1, the tetragonality of L7 is more pronounced compared to KL7 and the P-E hysteresis behavior is compatible with the XRD findings. The P-E hysteresis curve of 4 mol% Li added sample, on the other hand exhibits higher remnant polarization ( $P_r$ ) and lower coercive field values. However, the P-E curve is rather lossy.

The improvement that was obtained through changing the processing route in our study is thought to be mainly related to the stoichiometry and compositional homogeneity. The microstructural investigation of the samples also indicated a decreasing grain size through the R2 method for both 4 mol% and 7 mol% Li additions (Fig. 2). In the literature, the decrease of grain size is reported to have an effect on the extrinsic properties such as domain wall contribution to the electrical properties through increasing domain wall density and the clamping effect of increased grain boundaries [19,21,22]. However, a critical grain size of 1.5–2.0  $\mu\text{m}$  was reported, below which these effects were observed. In our case, although the grain size of the L4 and L7 samples decreased compared to their KL4 and KL7 counterparts, the grain sizes were still above the aforementioned critical grain size. Thus, the reduction of grain size as a result of changing processing method is not believed to be a source of improvement in the electromechanical properties.

## Conclusions

In this study, the effect of powder processing method on the electrical and, especially, electromechanical properties of lithium doped potassium sodium niobate piezoelectric ceramics were investigated. The Li doping ratio was set as 4 mol% and 7 mol%. Two different processing routes were used with the main difference being the calcination step. Compared to the loose-calcination route (R1), the ceramics fabricated using the compact-calcination route (R2) resulted in smaller grain size and better crystallinity for both Li doping ratios, and a higher tetragonality in the case of 7 mol% Li-doped samples. These structural changes were found to be reflected positively on the electrical properties of the ceramics. The remnant polarization ( $2P_r$ ) value of 7 mol% Li doped ceramic reached twice that of its original value and the coercive field ( $E_c$ ) was decreased to 2/3 of its original value as a result of the R2 processing route. The electromechanical properties were also found to increase 30% with the compact calcination route. These improvements are evaluated to be a result of the chemical homogeneity, i.e. more homogeneous ionic distribution and the intimate mixing that was obtained as a result of the compact calcination method.

---

## Acknowledgments

The authors would like to thank the financial support provided by the Turkish Academy of Sciences (TUBA) through the GEBIP-2013 Program.

---

## REFERENCES

---

- [1] Y. Saito, H. Takao, T. Tani, T. Nonoyama, K. Takatori, T. Homma, T. Nagaya, M. Nakamura, *Nature* 432 (2004) 84.
- [2] M.D. Maeder, D. Damjanovic, N. Setter, *J. Electroceram.* 13 (2004) 385.
- [3] E. Hollenstein, M. Davis, D. Damjanovic, N. Setter, *Appl. Phys. Lett.* 87 (2005) 187905.
- [4] L. Dunmin, K.W. Kwok, K.H. Lam, H.L.W. Chan, *J. Phys. D: Appl. Phys.* 40 (2007) 3500.
- [5] N.M. Hagh, K. Kerman, B. Jadian, A. Safari, *J. Eur. Ceram. Soc.* 29 (2009) 2325.
- [6] S. Wongsaenmai, S. Ananta, R. Yimnirun, *Ceram. Int.* 38 (2012) 147.
- [7] E.M. Alkoy, M. Papila, *Ceram. Int.* 36 (2010) 1921.
- [8] M. Matsubara, T. Yamaguchi, K. Kikuta, S. Hirano, *Jpn. J. Appl. Phys.* 44 (2005) 258.
- [9] E. Mensur Alkoy, A. Berksoy, S. Tekdas, *IEEE Trans. Ultrason. Ferroelectr. Freq. Control* 58 (2011) 1804.
- [10] E. Mensur-Alkoy, A. Berksoy-Yavuz, S. Alkoy, *Ferroelectrics* 447 (2013) 95.
- [11] E. Mensur-Alkoy, A. Berksoy-Yavuz, D. Avdan, S. Alkoy, *Proc. IEEE Int. Symp. on Applications of Ferroelectrics*, 2012, p. 274.
- [12] Y. Guo, K. Kakimoto, H. Ohsato, *Appl. Phys. Lett.* 85 (2004) 4121.
- [13] R.E. Newnham, *Properties of Materials*, vol. 87, Oxford University Press Inc., New York, 2005.
- [14] Z. Zhang, J. Yang, Z. Liu, Y. Li, *J. Alloys, J. Alloys Compd.* 624 (2015) 158–164.
- [15] A. Berksoy, E. Mensur-Alkoy, *Adv. Mater. Res.* 445 (2012) 492.
- [16] Y. Saito, H. Takao, *Ferroelectrics* 338 (2006) 17.
- [17] M. Hammer, M.J. Hoffmann, *J. Am. Ceram. Soc.* 81 (1998) 3277–3284.
- [18] V.S. Tiwari, D. Pandey, P. Groves, *J. Phys. D: Appl. Phys.* 22 (1989) 837–843.
- [19] C.A. Randall, N. Kim, J. Kucera, W. Cao, T.R. Shrout, *J. Am. Ceram. Soc.* 81 (1998) 677.
- [20] R.D. Shannon, *Acta Cryst. A* 32 (1976) 751.
- [21] C. Sakaki, B.L. Newalkar, S. Komarneni, K. Uchino, *Jpn. J. Appl. Phys.* 40 (2001) 6907.
- [22] F. Xu, S. Trolier-McKinstry, W. Ren, Xu. Baomin, Z.-L. Xie, K.J. Hemker, *J. Appl. Phys.* 89 (2001) 1336.